Performance analysis of integrated biomass gasification fuel cell (BGFC) and biomass gasification combined cycle (BGCC) systems

Jhuma Sadhukhan[1*], Yingru Zhao[2], Nilay Shah[3] and Nigel P Brandon[2]

[1]Centre for Process Integration, School of Chemical Engineering & Analytical Science, The University of Manchester, P. O. Box 88, Manchester, UK, M60 1QD

[2]Department of Earth Science and Engineering, Imperial College London, South Kensington Campus, London, UK, SW7 2AZ

[3]Centre for Process Systems Engineering, Imperial College London, South Kensington Campus, London, UK, SW7 2AZ

Abstract

Biomass gasification processes are more commonly integrated to gas turbine based combined heat and power (CHP) generation systems. However, efficiency can be greatly enhanced by the use of more advanced power generation technology such as solid oxide fuel cells (SOFC). The key objective of this work is to develop systematic site-wide process integration strategies, based on detailed process simulation in Aspen Plus, in view to improve heat recovery including waste heat, energy efficiency and cleaner operation, of biomass gasification fuel cell (BGFC) systems. The BGFC system considers integration of the exhaust gas as a source of steam and unreacted fuel from the SOFC to the steam gasifier, utilising biomass volatalised gases and tars, which is separately carried out from the combustion of the remaining char of the biomass in the presence of depleted air from the SOFC. The high grade process heat is utilised into direct heating of the process streams, e.g. heating of the syngas feed to the SOFC after cooling, condensation and ultra-cleaning with the Rectisol® process, using the hot product gas from the steam gasifier and heating of air to the SOFC using exhaust gas from the char combustor. The medium to low grade process heat is extracted into excess steam and hot water generation from the BGFC site. This study presents a comprehensive comparison of energetic and emission performances between BGFC and biomass gasification combined cycle (BGCC) systems, based on a 4th generation biomass waste resource, straws. The former integrated system provides as much as twice the power, than the latter. Furthermore, the performance of the integrated BGFC system is thoroughly analysed for a range of power generations, ~100-997 kW. Increasing power generation from a BGFC system decreases its power generation efficiency (69-63%), while increasing CHP generation efficiency (80-85%).

Keywords: biomass waste gasification, syngas fuel cell integration, gas turbine combined cycle, Aspen simulation, heat integration, energy efficiency

[*] Author/s to whom correspondence should be addressed:

E-mail: Jhuma.Sadhukhan@manchester.ac.uk, Ph: +44 161 306 4396, Fax: +44 161 236 7439

1. Introduction

Gasification of biomass waste has an important role to play in providing renewable energy to a broad range of sectors. Schemes can be applied to community or district level energy supply from a few dwellings to city-wide networks as well as to industrial sectors, as illustrated in the micro-generation manifesto, published by Green Alliance. Due to the localized availability of the biomass wastes, distributed CHP generation is an appropriate choice for end-use applications. Most of the biomass gasifiers operating for power generation today are combined either with gas engine or with gas turbine based combined cycles. The energy efficiency of a biomass gasification site can be greatly enhanced if coupled with high efficiency power generation systems, such as solid oxide fuel cell (SOFC). While biomass gasification combined cycle (BGCC) is a proven technology (Bridgwater et al., 2002; Craig and Mann, 1996), a fully integrated biomass gasification fuel cell (BGFC) is yet to be established.

Panopoulos et al. (2006) had studied the integration between an allothermal biomass gasifier and a SOFC, both operating at an atmospheric pressure, for small scale CHP generation, which was assessed by modelling in Aspen Plus process simulation software. The gasifier consisted of two fluidised bed reactors. The secondary gasification fluidised bed supplying heat to the primary gasification reactor, is fed with SOFC depleted off gases, un-reacted gasification char and additional biomass if required. Their integration study had analysed the lay out of heat pipes required for the thermal coupling between the two fluidised beds. A moderate level of electrical efficiency, 36%, was obtained, comparable to a BGCC system. Henceforth, there was no added advantage of replacing relatively low cost turbines with expensive, but high efficiency SOFC technologies. The thermal efficiency was at 14%. Nevertheless, electrical efficiency obtained is within a range as expected from a lower-cost BGCC system. Additionally, such a small scale CHP would have limited applications to residential installations, while an integrated BGFC system can also be applied to large scale district level generation of electricity and heat. Thus, there is a research need to achieve even higher efficiency and a greater consensus of such systems, for small scale as well as large scale biomass-to-CHP applications. In order to achieve highly efficient BGFC system designs for a wide range of applications, overall heat and

water integrated, energy efficient and cleaner process designs need to be developed, which is the main aim of this paper. Till date, no detailed and systematic analysis of material and energy flow pathways has been presented for overall integration and enhancement of efficiency of such systems. This study has also presented a comparison of energetic efficiency between newly developed highly efficient BGFC and more established BGCC systems.

SOFCs have the potential to become an energy technology in the UK and worldwide, due to their inherently clean and efficient operation. The SOFC can be used for community / district level generation of electricity and heat, e.g. a few hundred kilowatts to 1 megawatt of electricity, as well as in residential installations for around 1 kW of electricity generation, studied by Energy Saving Trust (community-heating-and-CHP) and the Office of Public Sector Information (OPSI) of the UK. Based on the green electrochemical principles, SOFCs work on reverse electrolysis process, oxidizing gaseous fuels such as hydrogen, syngas, etc. in the anode in the presence of an oxidant (air) in the cathode. Significant integration synergies in terms of process operating conditions and material and heat exchange, such as follows, may also exist between SOFC and biomass gasification processes, which could enhance the overall BGFC plant efficiency.

Operating conditions: Both gasifiers and SOFCs operate effectively at elevated temperatures of around 500–1000^{o}C and can be operated at atmospheric as well as elevated pressures. The SOFC for higher power generation can be operated at a higher pressure than atmosphere (e.g. 10 kW of power generation from a SOFC system operating at 3.5 bar pressure, Cresswell and Metcalfe, 2006), while pressurised gasifiers are a commonplace (Bridgwater et al., 2002; Craig and Mann, 1996). This provides opportunities for process integration.

Material integration: The nitrogen rich depleted air and exhaust gas from a SOFC are a good source of high temperature oxygen and steam, the two essential oxidising agents used in gasification processes. The BGFC system considers integration between the exhaust gas as a source of steam and unreacted fuel from the SOFC and the steam gasifier, utilising biomass volatalised gases and tars, which is separately carried out from the combustion of the remaining char of the biomass in the presence of depleted air from the SOFC. Additionally,

the SOFC has fuel flexibility, in which hydrogen, hydrocarbons and syngas can be used as feedstocks in principle. Even greater environmental benefits can be gained if gaseous fuels, such as syngas, which is a good source of renewable hydrogen, from biomass waste can be used as a fuel to the SOFC (Energy Saving Trust, community-heating-and-CHP).

Heat integration: To maximise the heat recovery from the product gas from the gasification process, a hot gas clean up strategy, followed by low temperature heat recovery via condensation of the gas below its dew point can be adopted. This leaves the gas dry and high in heating value, and hence ideal as a feed to the SOFC. The cold and dry product gas after ultra-cleaning to a trace level removal of contaminants discussed later, can itself be used to extract the heat from the hot syngas generating from the gasifier, before entering to the SOFC. Preheating the syngas and air fed to the SOFC to thermodynamically maximum achievable temperatures ensures maximum power generation efficiency from the SOFC. Preheating of feed gases facilitates endothermic reforming reactions and increases the net exothermic heat generation (due to combustion) from the SOFC. There are several other high temperature heat sources, such as exit gases from the SOFC. The excess heat from a highly integrated BGFC site can be recovered into high pressure superheated steam, which can further be utilised into additional power generation from the site.

In addition to the process integration challenges that exist between biomass gasification and SOFCs, a major hindrance to the commercialisation of a BGFC system is the stringent tolerance limits on the contaminants required for the SOFC feedstock (Panopoulos et al., 2006). The most common contaminant in the syngas feed to a SOFC is H_2S which originates from the raw materials used in gasification. It acts as a poison to the reforming and anode catalysts used in the SOFC. A tolerance limit as stringent as 0.1 ppm for H_2S in the SOFC feedstock has been reported to ensure thousands of hours of trouble free operation (Newby et al., 2001). The BGFC technologies in this work are developed based on a stringent biomass resource, straw (Kuramochi et al., 2005; Shen et al. 2008), hence they are expected to perform efficiently for similar or good quality biomass resource, such as (waste) wood. The Rectisol® technology developed by Lurgi that uses refrigerated methanol as the solvent for physical absorption / removal of undesired contaminants producing ultra-clean syngas is widely used in coal gasification plants (Koss and Meyer, 2002). Rectisol® provides an

excellent option for co-removal of a number of contaminants including H_2S, COS, HCN, NH_3, nickel and iron carbonyls, mercaptans, naphthalene, organic sulphides, etc. to a trace level (for e.g. H_2S to less than 0.1 ppm by volume), using one integrated plant, from stringent resources, like coal. Nearly each of the coal gasification units for the production of hydrogen or hydrogen rich gases and syngas with hydrogen and carbon monoxide as major constituents is equipped with a Rectisol® gas purification system. Because of the increasing use of biomass gasification technology in the face growing interest for chemical production, such as synthesis of ammonia, methanol, Fisher Tropsch liquids, oxo-alcohols, and gaseous products such as hydrogen, syngas, reduction gas and town gas, a steep increase in the application of Rectisol® processes is expected. A Rectisol® process needs to be integrated to a low temperature fuel gas, such that minimum cooling is needed to attain the required refrigeration for the Rectisol® process.

This paper takes the technological challenges into account in the development of novel process integration strategies for the deployment of a fully integrated BGFC plant using a 4th generation agricultural waste feedstock, straws, as the test case. The methodology comprises process simulation and heat integration of BGFC and BGCC systems in Aspen Plus, and electrochemical modelling to predict the power output from SOFC, illustrated in the following section. The results in terms of a comparison of the energetic, emission and performances between BGCC and BGFC systems are discussed in section 3. Important observations are summarised in section 4.

2. Methodology

2.1 Process integration strategies

There are significant synergies for simultaneous heat and material integration between the gasification and the SOFC systems, illustrated in Fig. 1, as follows.

Fig. 1

1) Design of the gasifier: The gasification process under consideration consists of two interconnected fluidised beds, a char combustor, combusting char in the presence of air, and a steam gasifier, gasifying biomass volatilised gases and tars (Shen et al., 2008). 'Direct contact between the gasification and combustion processes is avoided; the gasification-required heat is achieved by means of the circulation of bed particles. It is in a loop with end-to-end configuration composed of a circulating fluidized bed as a combustor, a cyclone, and a bubbling fluidized bed as a gasifier.' (Shen et al., 2008) This scheme avoids dilution of the resulting syngas with nitrogen whilst avoiding the use of an oxygen plant (air separation unit) for supplying pure oxygen to the gasifier. Panopoulos et al. (2006) have proposed a biomass allothermal fluidised bed gasifier comprising steam gasifier, tar cracker and combustor, operating at around 800^{o}C to produce a medium calorific value gas mixture, rich in H_2, CO, and CH_4, which are fuel species for SOFC. These schemes avoid dilution of the product gas with nitrogen whilst avoiding the use of an oxygen plant (air separation unit) for supplying pure oxygen to the gasifier. In view of the thoroughness of mixing and good gas-solid contact, the use of fluidised bed gasifiers is a commonplace (Craig and Mann, 1996). These designs have various advantages, such as relatively simple construction, greater tolerance to particle size range than fixed beds, good temperature control and high reaction rates, high carbon conversion, high specific capacity, high conversion efficiency, limited turndown and very good scale-up potential. In addition, only the fluid bed configurations are being considered in biomass applications that generate in a range and over 1 MWe (Overend and Rivard, 1993; Palonen et al., 1995). Atmospheric circulating fluid bed suppliers include TPS, Foster Wheeler, Battelle and Lurgi. Foster Wheeler has also developed a pressurised circulating fluid bed system.

2) Integration of syngas: The syngas rich in hydrogen and carbon monoxide from the steam gasifier, followed by cooling-condensation and ultra-cleaning using Rectisol®, is an excellent feedstock to the SOFC.

3) Syngas cleaning and heat recovery: The hot product gas clean-up and cooling comprise hot gas filtration for a removal of particulates, cooling or heat recovery and cleaning of contaminants to a trace level using the Rectisol® technology. The particulate-free hot gas is cooled down to preheat clean and dry syngas feed to the SOFC and to further generate superheated steam. These two heat recovery exercises can be done in parallel or series or combined within one heat exchanger unit. However, the hot gas coolers inherently require high maintenance, thus, introducing further complexity in the operation and maintenance in the latter case. Hence,

this study has been restricted to the case where preheating of clean and dry syngas feed to the SOFC and generation of superheated steam are performed in series, as depicted in Fig. 1. This is followed by a direct quench of the cold gas with cooling water below its dew point, so as to allow the separation of water and tar condensables from the remaining dry syngas. After sulphur and all other contaminants removal to a trace level using the Rectisol® process (Koss and Meyer, 2002), the ultra-clean and high heating value syngas rich in hydrogen is fed to the SOFC. The proposed scheme also recovers effluent water, which after waste water treatment and purge of sludge, can be fed back as boiler feed water (BFW) for steam generation within the BGFC system.

4) Steam from the SOFC: A SOFC produces high temperature steam, after electrochemically oxidizing hydrogen present in the syngas, while the gasification process requires such high grade steam, over and above that present as moisture in a biomass feedstock, thus adding more to the hydrogen concentration in the syngas feed to the SOFC. Steam gasification is essential to reform gas and tar and consequently reduce the tars. The tar, rich in phenol, can be reformed catalytically in the steam gasifier. Steam is also known to reduce the concentration of other forms of oxygenates including condensable (Craig and Mann, 1996). Thus part of the exhaust gas thus generated from the SOFC (anode) containing steam can be routed to the steam gasifier (Fig. 1). This also helps gasify any unreacted fuel from the SOFC. The total exhaust gas generating from the SOFC is divided between that emitted to atmosphere (after heat recovery, discussed later) to balance the carbon across a BGFC system and as a source of steam to the steam gasifier.

5) Steam generation from the SOFC exhaust gas cooler: The amount of the exhaust from the SOFC at a high temperature, not fed back as a source of steam to the steam gasifier, can be cooled (heat extracted) to generate superheated steam (from the waste heat boiler in Fig. 1). The water recovered from the product gas from the steam gasifier via the effluent treatment plant can be reused to recover this heat into superheated steam. A part of this steam can be routed to the steam gasifier to fulfil the balance of its minimum steam requirement. The rest of the steam is available as an excess steam from the BGFC site under consideration (Fig. 1).

6) Supply of air to the SOFC and gasifier processes: Both gasification and SOFC processes require oxygen (air). Oxygen needs to be added selectively at various gasification stages, such as in the secondary zones of a pyrolysis-cracker reactor, in order to preferentially oxidize tars. Its main role is to supply heat to the steam gasifier by combusting char in the char combustor. In a perfectly energy balanced BGFC flowsheet, the heat

from the char combustor must satisfy the heat requirements of the steam gasifier after the integration of the exhaust gas from the SOFC. The resulting depleted air from the SOFC cathode can thus be utilised as a source of oxygen in the char combustor. The amount of air to SOFC can be adjusted so as to maximise syngas fuel utilisation efficiency in the SOFC and consequently combust char in order to fulfil the heat requirement of the steam gasifier (Fig. 1).

7) Feed preheating: The air and syngas feedstocks need preheating before entering to the SOFC, so as to avoid thermal shock of the ceramic components and such that the sensible heat in them can be made available for power generation through electrochemical process from the SOFC. Either of the exhaust gases from the char combustor and / or the SOFC can be used to preheat air. From the heat integration point of view, a heat exchange between the exhaust gas from the char combustor and air is preferred, based on a closer match of the heat capacities between the two streams. The hot gas directly from the gasifier can not be fed to the SOFC at the gasifier temperature, without thorough quench with cooling water. In order to avoid this heat loss, heat from the hot and moist gas from the gasifier is recovered into preheating the clean and dry syngas product, fed to the SOFC as shown in Fig. 1.

8) Excess steam: An overall BGFC site can be a net generator of heat. Excess heat in the form of superheated steam can be generated utilising hot product gas from the steam gasifier in the superheater and a part of the hot exhaust gas from the SOFC in the waste heat boiler, respectively, as shown in Fig. 1.

9) Low grade heat: The various sources of low grade heat include heat of condensation of the SOFC exhaust gas, hot water recovered via condensation of the SOFC exhaust gas and low temperature sensible heat from the exhaust gas from the char combustor. Whether the low grade heat recovery is cost-effective or not depends on the amount of low grade heat generation, which obviously is more justifiable for higher capacity BGFC sites, further illustrated in the results and discussion section.

2.2 Aspen simulation of integrated BGFC flowsheets

The process operating conditions of a BGFC site are first illustrated, in this section. The additional process operating conditions of a BGCC site are highlighted thereafter. Simulation of the integrated BGFC flowsheet, discussed previously in view to improve energy efficiency, heat recovery and cleaner operation, in Fig. 1, is

undertaken in Aspen Plus, depicted in Fig. 2. The basis of the energy efficiency studies for the integrated BGFC system is a power generation of > 600 kW from the SOFC, based on 85% clean syngas utilisation in the SOFC. To generate 652.61 kW of electricity from the SOFC, 9.13 t/d of clean syngas feed needs to be produced from 5.44 t/d of straw slurry, the ultimate analysis of which is provided in Table 1. The same basis for feedstock flowrates is used in simulation of the BGCC system. Tables 2-3 provide the specifications of streams and processes and results (compositional and thermal) obtained from Aspen simulation presented in Fig. 2, respectively. The SOFC for this range of power generation can be operated at around 5 bar. The same or slightly lower pressure can also be maintained in the biomass gasifier. The ambient temperature is assumed to be 25^{o}C.

The two reactors in the interconnected circulating fluidised bed gasifier (Shen et al., 2008) shown in Fig. 1 are simulated as RGibbs reactors, STGASIFY, fed with gas (GASIN) and tar (TARIN), and CHAR-RCT, fed with char (CHARIN) and ash (ASH), respectively (Fig. 2). These streams are derived from primary pyrolysis of a biomass feedstock, provided in Tables 1a-b. The primary pyrolysis occurs as soon as a biomass feedstock comes in contact with the hot bed within a gasifier before any mixing / mass transfer / chemical reaction with other reactants, steam and oxygen, takes place in a gasifier. Researchers have found better representations of gasification processes by dealing with the primary pyrolysis products of a biomass feedstock (Table 1b) (Peijun et al., 2009). The composition of GASIN and the amounts of GASIN, TARIN and CHARIN, in Table 3 were predicted using the ultimate analysis of straws in Table 1a and correlations provided in Table 1b. TARIN has been presented as phenol as its major constituent, as revealed in numerous studies (Gerun et al., 2008; Peijun et al., 2009), while CHARIN and ASH were modelled as non-conventional components. The compositions of GASIN, TARIN, CHARIN and ASH are thus determined to balance with the C, H, N, O, S, ash and moisture contents in a biomass (Tables 1a-b and 3). The Non-Random Two Liquid (NRTL) thermodynamic package was used for the properties estimation. The SOFC unit comprises of a cathode (CATHODE) and an anode (ANODE), modelled as a two component separator (Sep2) with 95% efficiency and a Gibbs reactor (RGibbs), respectively, in Table 2.

Fig. 2

Table 1

Table 2

Table 3

A BGFC site can be a good source of heat with both the gasifier and SOFC operating at high temperatures. It has been observed that with increasing temperature and at lower pressure of the gasifier, the concentration of hydrogen in the syngas increases, hence, the heating value of the syngas increases. However, a higher temperature, >1000^{o}C, may cause operational difficulties and maintenance problems, while increasing pressure is associated with increased power generation from gas turbines in case of the BGFC system. SOFCs operate at elevated temperatures of around 500–1000^{o}C and therefore can be a good source of high grade heat (Hawkes et al., 2007). In the case studies presented here, the gasifier and SOFC temperatures are maintained at 950^{o}C and 800^{o}C respectively (Table 2). The pressure in SOFC may be varied from atmospheric to ~10 bar for 1 kW to 1 MW power generation, respectively, illustrated in the scenario analysis in the results and discussion section.

Fig. 2 depicts the gas clean-up processes that comprise hot gas filtration (CYCLONE) for the removal of particulates, flash separator (EFFLUSEP) for condensation of water and other condensates (e.g. tar) (WATERREC), from the gas by cooling the gas below its dew point and the Rectisol® process, modelled as a two component separation unit (H2SREMOV) operating at 99% efficiency, respectively. The following utility consumptions are established for the Rectisol® process (Kohl and Neilsen, 1997): shaft power: 73.08 kW, LP steam: 323.74 kW and refrigeration duty: 131.42 kW, respectively, per kmol/hr of sulphur and nitrogen compounds removed, where total kmol/hr sulphur and nitrogen compounds removed calculated from the inlet and the outlet stream analyses, 1 and SYN2SOFC, respectively (Table 3). The Rectisol® process can also be operated at low syngas capacity, ~355 Nm^3/hr, as demonstrated in Shanghai Coking & Chemical Corportation plant (Linde Engineering, 2005). In this case, the syngas capacity is ~390 Nm^3/hr. The clean and dry syngas, SYN2SOFC, (and after preheating, ANODFUEL) has almost equal molar compositions of hydrogen and carbon monoxide (32.8% each), both of which are combustible in the SOFC. Based on 85% of the total enthalpy change from SYN2SOFC and O2RICH, fed to the SOFC anode, to FLU2GASI, produced from the

SOFC anode, the electricity generation for the base case simulation provided in Table 3 is 652.61 kW. Alternatively, 85% of the heat of combustion of hydrogen and carbon monoxide can also be taken into account to predict the electricity generation from the SOFC.

A key energy efficiency exercise consists of heat integration between hot-cold process streams or coolers-heaters, governed by thermodynamic optimality or maximum heat recovery strategy (Smith, 2005) and identification of basic processing chains to aid with process decision making and establish mass and energy balance, as follows.

2.3 Heat integration of BGFC flowsheets

Once the temperature, pressure and stream compositions are decided for the major process units (e.g. reactors and separators), coolers and heaters are placed on the hot and cold streams respectively to achieve their respective target temperatures (Tables 2-3). Next, the best thermodynamic matching or process to process heat integration between the coolers and heaters is obtained as follows (indicated by dotted lines joining respective cooler-heater in Fig. 2).

Two heat recovery strategies can be straightway adopted from conventional IGCC systems (Sadhukhan and Zhu, 2002): syngas cooling and heat recovery from the exhaust gases, into the generation (economiser and evaporation) and superheating of steam. Additionally, the site has a major high temperature heat requirement for preheating SYN2SOFC from 25^{o}C up to the operating temperature of the SOFC, 800^{o}C, which can only be satisfied by the high temperature (950^{o}C) heat available in SYN2COOL (Fig. 2 and Table 3). Hence, a heat exchange between SYNGCOOL (cooler) and FUELHEAT (heater) is an obvious choice for process integration. After preheating SYN2SOFC to 800^{o}C, the medium grade heat remained in SYN2COOL (450^{o}C to the dew point of the gas) can then be utilised in the generation of superheated steam (stream 12 at 300^{o}C and 5 bar, Table 3) from BFW, in unit B3, in Fig. 2.

Similar to the syngas feed to the SOFC, air also needs preheating, after compression (AIRCOMPR), up to a maximum temperature of the SOFC, 800^{o}C. The two sources of exhaust gas are from the SOFC and the char combustor, EXHAUSTI (at 800^{o}C) from ANODE and CHARPDT (at 950^{o}C) from CHAR-RCT, respectively, from which the high grade heat can be recovered into superheated steam and / or to preheat air. As CHARPDT provides a feasible temperature driving force for maximum preheating of air (upto 800^{o}C), and also based on closer match of the heat capacities between the CHARPDT and AIR2CATH-19 streams, thermal integration between AIRHOT (cooler) and AIRCOLD (heater) is thermodynamically more favourable (Figs. 2-3). Fig. 3 provides the enthalpy change of the hot stream (CHARPDT) and the cold stream (2) over the temperature range in AIRHOT-AIRCOLD exchanger, and ensures that there is no temperature cross-over between the two. The inlet temperature of the air from the air compressor (AIRCOMPR operating at 75% efficiency, Table 2) to AIRCOLD is 245^{o}C. A minimum temperature approach of 35^{o}C occurs at the inlet of the air and outlet of EXHAUST, in a counter-current exchanger, for achieving the maximum air preheating. Finally, WATERHOT and WATERCOL are combined for exhaust gas heat recovery (down to 85^{o}C or the dew point of the exhaust gas, stream 17) to superheat steam, stream 5 (at 320^{o}C and 5 bar from 25^{o}C), in Fig. 2 and Table 3, following the strategy adopted in conventional IGCC processes (Sadhukhan and Zhu). Thus, these pairs constitute the major exchangers for a high grade process to process heat recovery in a BGFC site.

Fig. 3

2.4 Analysis of processing chains in BGFC flowsheets

Based on the discussions above, four main processing chains in the integrated BGFC system can be identified to help in decision making, illustrated as follows (Fig. 2 and Tables 2-3).

1) TARIN-GASIN-GASPDT-SYN2COOL-27-8-1-CLEANSYN-SYN2SOFC-ANODFUEL-FLU2GASI-EXHAUSTI-STGASIFY-17-20-15-16: Key decision makings in this processing chain involve heat recovery from the hot and unclean gas from the steam gasifier, GASPDT or SYN2COOL and preheating of SYN2SOFC, already discussed, and waste heat recovery from EXHAUSTI and recycling of STGASIFY. From the component balance, the carbon intake through TARIN and GASIN should be released to the

atmosphere via the stream 15. Hence, a split ratio of EXHAUSTI of 60.9% of FLU2GASI can be decided in B7 to maintain the carbon balance in this processing chain (Table 2). The waste heat content in the EXHAUSTI can be recovered into economising, evaporating and superheating the water recovered (stream 7 in Table 3) from the effluent treatment unit into superheated steam generation (stream 5). The steam content in the recycle stream, STGASIFY, enhances the hydrogen concentration in the syngas, while its unreacted hydrogen and carbon monoxide can provide a better balance between the endothermic steam gasification and exothermic char combustion reactions, resulting into an overall thermally neutral gasification process operation, further illustrated in the results and discussion section.

2) WATERREC-7-PURGEH2O-5-STEAMIN2-3: The main decision making involved in this processing chain are the conditions of steam to be generated and the amount of steam to be recycled back to the STGASIFY process. It is recommended that a steam to biomass weight ratio of 0.6 is used in the gasification processes in order to ensure a good mixing and conversion (Shen et al., 2008). The flowrate of STEAMIN2 thus decided to achieve this recommended steam to biomass ratio. With respect to BFW balance, after 10% purge of sludge waste, the BFW recovered is recycled as superheated steam, STEAMIN2 to STGASIFY and the excess superheated steam, 3, is generated from the site, which can be utilised into CHP generation. The steam temperature and pressure conditions of STEAMIN2 and 3 thus become a variable to adjust against the excess amount of steam generation. Steam conditions with lower than 300^{o}C temperature was not recommended in order to avoid any thermal shock in the steam gasifier, STGASIFY.

The two processing chains discussed above are closely interlinked via steam balance. The pairing of WATERHOT-WATERCOLD determines the conditions of the steam generation. Additionally, the flowrates of the excess steam 3 and the recycle stream STGASIFY are interdependent, and any change in either of their flowrates affects the conditions of the steam entering to the STGASIFY unit, hence, the hydrogen and carbon monoxide concentrations in the syngas feed to the SOFC and overall performance of the SOFC. Therefore, extreme conditions are further investigated and a comparison against the base case is presented in the results and discussion section.

3) AIR2CATH-2-19-O2RICH-N2CHARCT-CHARPDT-EXHAUST-11: This route has relatively less flexibility in varying the operating conditions, as long as the type and flowrate of the biomass feedstock to the system are fixed. The quantity of air was decided to ensure complete combustion in the char reactor and maximum fuel utilisation of the syngas in the SOFC. The heat integration between AIRCOLD and AIRHOT is already discussed. The low grade heat available from the char combustor waste heat recovery unit, CHCOMXCW, remains unchanged, irrespective of any modification in the first two processing chains discussed, for the same biomass flowrate.

4) BFW-12-3-18-13: This is the route for the utilisation of the excess steam in CHP generation. The excess steam can generate power only in a few kW range (micro-turbine). The micro-turbines are a great research challenge and their investment can only be justified for the higher range of power generation. An alternative is to produce the entire superheated steam, as a source of high grade heat (stream 18 at 304^{o}C and 5 bar in Table 3).

A BGFC site also generates a considerable amount of low grade heat as highlighted in Table 4. The low grade heat can be obtained from the cooling of the char combustor exhaust gas (CHCOMXCW) and condensation of the SOFC exhaust gas below the dew point (SOFCXCW) using cooling water, hot water / condensate recovered from the SOFC exhaust (16 from the Flash separator, B14) and the low pressure steam extracted from the steam turbine (stream 13 from STEAMTUR), respectively (Fig. 2). The shaded areas in Table 4 highlight the energy consumption of the Rectisol® and the Selexol® processes. A detailed energetic analysis provided in Table 4 is further illustrated in the results and discussion section.

Table 4

2.5 Aspen simulation of integrated BGCC flowsheets

The simulation framework developed for the BGCC system for the same basis (9.13 t/d of clean syngas feed or 5.44 t/d of straw slurry) is presented in Fig. 4. The upstream processes, such as gasification (Fig. 1), gas

cooling and cleaning processes, are common to both BGFC and BGCC flowsheets (Figs. 2 and 4 respectively). Therefore, only the additional features of simulation of a BGCC system are presented here. A pressurised gasifier, e.g. 30 bar can be considered, as increased pressure is associated with increased power generation from the gas turbines in a BGCC system (Bridgwater et al., 2002; Craig and Mann, 1996). The exhaust gas (rich in N_2 and CO_2) from the air driven char combustor is added to the product gas from steam gasifier in order to maximize the heat recovery into superheated steam and hence power generation. This exhaust gas can also act as an inert gas to compensate for the lost effluent from the dry feed gas to gas turbines, thereby, adjusting the heating value of the gas turbine fuel. The lower temperature of the gas feed to the gas turbines minimises the temperature rise in the gas turbine combustor, and consequently the NO_x emission. A Selexol® process of UOP, in the place of the Rectisol® process can be used due to the requirement of less stringent syngas fuel specification to gas turbines (e.g. H_2S in the range of 1 ppm) (Koss and Meyer, 2002). The Selexol® process, unlike the Rectisol® process, is less energy intensive requiring only steam and no refrigeration. The Selexol® process is modelled as a separator in Fig. 4. The low pressure steam required for the Selexol® process was established (Table 4) using simulation of the Selexol® process presented elsewhere (Lou, 2008). A BGCC system additionally comprises gas turbines, heat recovery steam generators (HRSG) and steam turbine networks. The air compressor and gas turbine expander are modelled as power consumption and generation units respectively, with 75% isentropic efficiency, while the combustion section in the gas turbine is modelled as a Gibbs reactor. The generation of superheated steam at a temperature of 550^oC and a pressure of 65 bar from the gas cooler and power generation using all excess steam through back pressure steam turbines are considered. A detailed comparison of energetic analysis between BGFC and BGCC systems established from the Aspen simulation is presented in Table 4 and further illustrated in the results and discussion section.

Fig. 4

2.6 Electrochemical modelling of SOFC

This section provides the model for predicting electrical output from a SOFC. The basic working principle of a solid oxide fuel cell is presented in the following. The air is taken to the cathode of a SOFC, where oxygen ions are generated and migrate to the anode through the electrolyte. In the anode, fuel gas is oxidized releasing electrons to the external circuit and hence to the cathode and producing water. The nitrogen rich depleted air and exhaust gas are resulted from the cathode and anode of a SOFC respectively. A SOFC has high electrical as well as CHP generation efficiency.

The various chemical reaction kinetic parameters obtained from the Aspen simulation, as presented in Table 5, are used in electrochemical modelling of the SOFC to predict its output power generation. The main feed and product streams to the SOFC cathode and anode are 19, N2CHARCT and ANODFUEL and FLU2GASI, respectively, as depicted in Fig. 2. The data that need to be collated from the Aspen simulation results in Table 3 for predicting electrochemical output of the SOFC unit include compositions, flowrates and molar enthalpy and entropy of these feed and product streams. Previous studies have neglected the impact of the presence of the reacting species e.g. carbon monoxide, methane in syngas, other than hydrogen on the power output (Janardhanan and Deutschmann, 2007). We have taken account of all the reacting species (carbon monoxide and methane) and non-reacting species (carbon dioxide, steam, and traces of all other components) to replace the partial pressures of hydrogen and steam, P_{H_2} and P_{H_2O}, respectively, in the model provided in Eqs. 1-4. The enthalpy and entropy changes are also corrected to Aspen simulation results. A steady state irreversible model in Eqs. 1-4, provided by Zhao et al. (2008), was used to predict the amount of power generation from the SOFC. The other parameters used in the SOFC electrochemical model (Eqs. 1-4) are given in Table 5. The SOFC output voltage is less than the reversible cell voltage because there are voltage drops across the cell caused by irreversible losses. The electrochemical model takes account of such losses due to activation, ohmic and concentration overpotential.

Table 5

Power output and efficiency of the fuel cell (Zhao et al., 2008):

$$P_{fc} = \frac{iA}{n_e F}\left(m - \frac{k}{RTd_1}m^2\right) \quad \text{(Eq. 1)}$$

$$\eta_{fc} = \frac{P_{fc}}{-\frac{iA}{n_e F}\Delta h^\circ} = \frac{1}{-\Delta h^\circ}\left(m - \frac{k}{RTd_1}m^2\right) \quad \text{(Eq. 2)}$$

Where $d_1 = 2n_e \sinh^{-1}\left(\frac{i}{2i_{0,a}}\right) + 2n_e \sinh^{-1}\left(\frac{i}{2i_{0,c}}\right) - \ln\left(1 - \frac{i}{i_{L,a}}\right) - \ln\left(1 - \frac{i}{i_{L,c}}\right) + \frac{in_e FL_{el}}{\sigma_0 R}\exp\left(\frac{E_{el}}{RT}\right)$, $k = R_{int} / R_{leak}$, and

$m = -\Delta h^\circ + T\Delta s^\circ + RT\ln\left(\frac{p_{H_2} p_{O_2}^{1/2}}{p_{H_2O}}\right) - RTd_1$.

The terms in d_1 from left hand side to right hand side indicate the voltage drops across anode and cathode caused by activation overpotential (the first two terms), concentration overpotential (the second two terms) and Ohmic overpotential (the last term) respectively. i is the current density, F =96485 C mol^{-1} is Faraday's constant, R =8.314 J mol^{-1} K^{-1} is the universal gas constant. n_e is the number of electrons participating in the reaction. A is the surface area of the fuel cell plate, Δh° and Δs° are the standard molar enthalpy and entropy changes of the reaction at temperature T, respectively, k denotes the ratio of the equivalent leakage resistance to the internal resistance of the fuel cell and is assumed to be a constant. L_{el} is the thickness of electrolyte, E_{el} represents the activation energy for ion transport, and σ_0 is the reference ionic conductivity. p_0 is the ambient pressure, p_{H_2}, p_{O_2} and p_{H_2O} are the partial pressures of reactants, O_2 and non-reacting components, respectively. $i_{L,a}$ and $i_{L,c}$ are the limiting current densities of the anode and cathode, respectively. The anode and cathode exchange current densities, $i_{0,a}$ and $i_{0,c}$, are calculated using Eqs. 3-4 (Zhao et al., 2008) respectively and the rest of the parameters present in Eqs. 1-2 have either fixed values or obtained from Aspen simulation, as provided in Table 5. Table 5 also contains the nomenclature of the parameters used.

$$i_{0,a} = \gamma_a\left(\frac{p_{H_2}}{p_0}\right)\left(\frac{p_{H_2O}}{p_0}\right)\exp\left(-\frac{E_{act,a}}{RT}\right) \quad \text{(Eq. 3)}$$

$$i_{0,c} = \gamma_c\left(\frac{p_{O_2}}{p_0}\right)^{1/4}\exp\left(-\frac{E_{act,c}}{RT}\right) \quad \text{(Eq. 4)}$$

γ_a and γ_c are pre-exponential coefficients for the anode and cathode, respectively. $E_{act,a}$ and $E_{act,c}$ are activation energies for the anode and cathode, respectively. Using Eqs 1-4 and parameters provided in Table 5, the current density cross the fuel cell, *iA*, predicted is 371.72 Amp, based on 85% efficiency of the SOFC (Eq. 2).

3. Results and discussions

Table 4 presents energetic analysis of the base case of the integrated BGFC site in Fig. 2 and Tables 2-3 and the BGCC site under consideration (Fig. 4), respectively. The net power generation, 601.89 kW and 295.60 kW, are calculated from the power generation from the SOFC (652.61 kW) and gas turbines (192 kW) and steam turbines (9.43 kW and 234.66 kW), subtracting by the power consumption by compressors (58.05 kW and 131.06 kW) and other processes, (e.g. the Rectisol® process requires a shaft power of 0.75 kW, and refrigeration duty of 1.35 kW in the BGFC system), for the BGFC and BGCC systems, respectively (Table 4). The electrical efficiency of 64.41% of the BGFC system however does not include the power generation from the steam turbines, and this energy is made available as excess steam from the system. The BGCC system achieves an energy efficiency of 32.14%. The efficiencies are based on the biomass LHV calculated from Table 1a, 919.79 kW. The corresponding CHP generation efficiencies, 83.4% and 42.23%, include the heat generations / consumptions from the respective sites, such as, waste heat recovery from the exhaust gases, 47.48 kW + 2.8 kW + 1.29 kW (sensible heats) and 31.18 kW (heats of condensation) from the BGFC system and 93.57 kW from the BGCC system; LP steam generation (95.18 kW from the BGFC site) and consumption, 3.33 kW from the BGFC and 0.75 kW from the BGCC systems. Condensation of the SOFC exhaust gas emitted to atmosphere is considered to recover hot water from the gas at 50^{o}C, hence, both the heat of condensation of the gas (31.18 kW) and the enthalpy in the hot water recovered on the basis of 25^{o}C (1.29 kW) are taken into account. In all cases, 25^{o}C and atmospheric pressure are assumed as the basis for the calculation of enthalpies in the Aspen simulation. It can be noted that the hot water generated from a SOFC is in a very pure form and can be utilised in heat applications without any purification. The CHP generation efficiency of the BGFC case is significantly higher, even without any consideration of heat recovery from the

SOFC exhaust gas emitted (79.63%). Hence, an integrated BGFC system can provide twice as much power, compared to an integrated BGCC system.

The end-of-pipe emission performance of a BGFC plant is far superior to a BGCC plant, with the former incurs less than 0.1 ppm by volume emissions of individual components: H_2S, COS, HCN, NH_3, nickel and iron carbonyls, mercaptans, naphthalene, organic sulphides, etc., compared to less than 1 ppm by volume of individual emissions from the latter case. This is due to the difference in performance between the Rectisol® and the Selexol® processes.

Next, the key decision making involved in the four main processing chains indentified in the integrated BGFC system in Fig. 2 is discussed as follows. The performance of the proposed integrated BGFC flowsheet is evaluated for a range of power ratings and the design tradeoffs are analysed.

1) TARIN-GASIN-GASPDT-SYN2COOL-27-8-1-CLEANSYN-SYN2SOFC-ANODFUEL-FLU2GASI-EXHAUSTI-STGASIFY-17-20-15-16: The unreacted hydrogen and carbon monoxide in STGASIFY routed to the steam gasifier (due to 15% unutilised fuel present in FLU2GASI from the SOFC) provide additional heat to the steam gasification reactions. Based on 15% unutilised hydrogen and carbon monoxide in STGASIFY, an additional 115.17 kW of heat can be made available to the steam gasifier. Hence, this integration provides a conservative balance between the endothermic steam gasification and exothermic char combustion reactions, 48.79 kW and 35.5 kW respectively, as obtained from Aspen simulation. It can be noted that the endothermic heat of steam gasification reactions obtained from the computer simulation depends on the way tar has been defined. For example, if tar is defined as benzene (Mermelstein et al., 2009), an additional 74.09 kW of endothermic heat of reaction would be required for its steam gasification (e.g. cracking, reforming). Hence, a conservative approach to fuel utilisation in the SOFC has been considered to ensure the desired thermally neutral performance of the overall gasification process. With tar defined as benzene, 3% more molar concentrations of each of hydrogen and carbon monoxide in the syngas feed to the SOFC (ANODFUEL in Table 3) are obtained, providing a higher heating value of the inlet feed and hence power generation from the SOFC. This is compensated by the requirement of a higher endothermic heat of

steam gasification reaction. Thus, 85% utilisation of the syngas fuel to the SOFC is a safe assumption, providing enough marginal heat for facilitating the steam gasification reactions of tar, irrespective of how it is specified.

2) WATERREC-7-PURGEH2O-5-STEAMIN2-3: For the given conditions of superheated steam generation at 320^{o}C temperature and 5 bar pressure from WATERCOL, the following BFW balance is determined after 10% purge of the sludge (Table 3): 1.994 t/d of recycle steam, STEAMIN2, to the steam gasifier unit and 0.613 t/d of the excess steam, 3.

One extreme case can also be considered, where there is no excess steam generation through the processing chain WATERREC-7-PURGEH2O-5-STEAMIN2-3. The amount of steam supply, STEAMIN2, to the STGASIFY unit is thus increased from 1.994 t/d (Table 2) to 2.58 t/d for the given purge ratio of 10% from the waste water treatment unit. This increases the flowrate of EXHAUSTI to 74% of FLU2GASI, compared to 60.9% in the base case in Table 2, while keeping the same steam to biomass weight ratio at 0.6. The increased heat availability (100 kW) from WATERHOT can be utilised into an enhanced superheating steam condition to 500^{o}C from WATERCOL. The overall effect is an increase in hydrogen concentration in ANODFUEL to the SOFC, 41% compared to 33% in Table 3, and hence, increased power generation to 666 kW from the SOFC (based on 85% fuel utilisation efficiency). A comparison of stream variables and enthalpy balance between the base case in Tables 2-4 and the case with maximum recycling of steam recovered from gas cooling, to gasification is presented in Table 6. The values of the independent variables, flowrates of streams 3, STEAMIN2 and EXHAUSTI (Fig. 2), are shown in shaded areas in Table 6.

Table 6

The overall heat balance around the gasification unit shows the following new set of endothermic heat of steam gasification reactions, exothermic heat of char combustion reactions and heat generation from 15% unutilised syngas fuel from the SOFC, 57.64 kW, 35.5 kW and 118.45 kW, respectively. With the modified conditions in Table 6, a lesser amount of excess steam, 18, of 79.5 kW from B3 is generated. This is

compensated by an increased availability of 17.58 kW of waste heat recovery from the SOFC emission route, EXHAUSTI-17-20-15-16. The difference in the net energy generation from the site is 5.47 kW more using the new set of operating conditions given in Table 6. This amount of heat is then no longer available from the overall exothermic performance of the gasifier, making its design less conservative, compared to the base case.

3) AIR2CATH-2-19-O2RICH-N2CHARCT-CHARPDT-EXHAUST-11: The air compressor consumes 58.05 kW based on 75% isentropic efficiency in both the cases illustrated in Table 6. The low grade heat available from the char combustor waste heat recovery unit, CHCOMXCW, remains the same at 47.48 kW, for the same basis of the biomass feedstock (Table 4).

4) BFW-12-3-18-13: Simulation of the base case shows a power generation of 9.43 kW from a back pressure steam turbine STEAMTUR, while the useful enthalpy available in the steam, 13, at 168^{o}C and 1 bar is 95.18 kW (Table 4). Alternatively, the superheated steam, 18, at 304^{o}C and 5 bar can be made available as a source of high grade heat, 104.61 kW (Tables 3 and 6).

In addition to the analysis of the processing chains in the integrated BGFC system in Fig. 2, a comprehensive energetic performance for two different ratings of electricity generation from the SOFC, ~100 and 1000 kW, 100.41 kW and 996.68 kW from the simulation cases, respectively, is also presented in Table 7. For these electricity ratings, the corresponding SOFC operating pressures are 2 and 7 bar, respectively. Hence, the overall system pressure is also set at these pressures, respectively. The intake of biomass and air to the BGFC system was proportionally reduced by 0.154 times and enhanced by 1.53 times in order to achieve 100.41 kW and 996.68 kW of SOFC electrical outputs from 652.61 kW, respectively. The amounts in kg/s of TARIN, GASIN, CHARIN and ASH predicted using correlations provided in Table 1b, are 15, 15.31, 1.27 and 3 for 100.41 kW and 149.22, 152.26, 12.59 and 29.88 for 996.68 kW of SOFC electrical outputs respectively.

Table 7

The net electrical output from a BGFC system depicted in Figs. 1-2 is the electricity generation from the SOFC, subtracting by the electricity consumption by the air compressor and the Rectisol® process (Table 7). The corresponding LHV of the feedstock was taken into account to predict the net electrical efficiency of the system, which was found to increase with the decrease in the SOFC electrical output. For example, as the SOFC electrical output increases from 100.41 kW through 652.61 kW (Table 4) to 996.68 kW, the electrical efficiency decreases from 68.46% through 64.41% to 62.61%, respectively. The net electricity outputs are 96.87 kW, 592.46 kW and 881.04 kW, respectively. The decrease in the net electrical efficiency with increasing electrical output is due to much increased electricity consumption for increased load by the air compressor. As the air compression ratio increases from 2 to 5 and 7 bar, the electricity consumption increases by 18 times (from 3.22 kW to 58.05 kW, Tables 7 and 4) and 35.5 times (from 3.22 kW to 114.27 kW, Tables 7 and 4), respectively.

In contrary, the benefits due to heat generation are predominant for the higher net electrical output, resulting into 84.78% and 79.96% CHP generation efficiency for 996.68 kW and 100.41 kW of SOFC electrical outputs, respectively. This is because the low grade waste heat from the exhaust of the char combustor (cooler CHCOMXCW) and the SOFC (B11-B14-16 in Fig. 2) may not be cost-effective to recover when their heat available is insignificant, 2.1 and 5.4 respectively, and hence is neglected, for the lower electrical output 100.41 kW case (Table 7). The corresponding low grade heat recoveries are 47.48 kW and 7.27 kW for 652.61 kW, and 96.5 kW and 53.53 kW for 996.68 kW SOFC electrical outputs, respectively. With the inclusion of this low grade heat, the net CHP generation efficiency for the case with SOFC electrical output of 100.41 kW can go up to 85.25%. In addition, heat duties of the three major exchangers: air preheater (AIRHOT-AIRCOLD), steam economiser-evaporator-superheater (WATERHOT-WATERCOL) and the syngas pre-heater to the SOFC (SYNGCOOL-FUELHEAT) in the integrated BGFC system demonstrate an equivalent increase in the process to process heat recovery, from 62.25 kW to 545 kW, with the increase in SOFC electrical output, from 100.41 kW to 996.68 kW, respectively. The minimum temperature approach in the air pre-heater is lower at 20^{o}C in the case with lower electrical output.

4. Conclusions

This paper establishes a process simulation and integration based methodology for the integrated design of biomass gasification fuel cell systems and for energetic the comparison of these systems with biomass gasification combined cycle systems. Extensive integration strategies between biomass gasification and fuel cells have been established based on maximum heat recovery including waste heat, material utilisation and power generation objectives. These include integration of syngas from the gasifier to the SOFC, exhaust gas (rich in steam and with unreacted fuel gases, hydrogen and carbon monoxide) and depleted air from the SOFC to the steam gasifier and various other indirect (gas coolers, SOFC and char combustor exhaust gas coolers and SOFC feed gas preheaters) and direct heat recoveries (e.g. heat of condensation of the SOFC exhaust gas emitted to the atmosphere). With this respect, the BGFC system was identified to have four major processing chains, material and heat balance around which helps with the following decision making: 1) flowrate of the SOFC exhaust gas to be recycled as a source of steam to the steam gasifier and that emitted to the atmosphere; 2) indirect heat recovery from the SOFC exhaust gas emitted, into the generation of superheated steam for meeting the balance of the steam required by the gasifier and establishing excess steam generation; 3) heat and material integration between SOFC and char combustor via air; 4) excess steam generation by indirect high temperature heat recovery from the hot gas. A base case BGFC site is established for 650 kW of power generation from the SOFC. This case is further evaluated for an extreme scenario, where all steam generating using BFW recovered from gas condensation and by indirect heat recovery from the SOFC exhaust gas emitted to the atmosphere, are used in the steam gasifier. Furthermore, the proposed BGFC system is evaluated for ~ 100 kW and ~ 1000 kW of power generations, which have been found to strongly influence the power and CHP generation efficiencies of the site in two opposing ways. The integrated BGFC system is established to have twice as much power generation potential than an integrated BGCC system.

References

Bridgwater, A.V., Toft, A.J., Brammer, J.G., 2002. A Techno-economic comparison of power production by biomass fast pyrolysis with gasification and combustion. Renewable and Sustainable Energy Reviews 6, 181-248.

Craig, K.R., Mann, M.K., 1996. Cost and Performance Analysis of Biomass-Based Integrated Gasification Combined-Cycle (BIGCC) Power Systems. National Renewable Energy Laboratory Report NREL/TP-430-21657.

Cresswell, D.L., Metcalfe, I.S., 2006. Energy integration strategies for solid oxide fuel cell systems. Solid State Ionics 177, 19-25, 1905-1910.

Gerun, L., Paraschiv, M., Vîjeu, R., Bellettre, J., Tazerout, M., GBbel, B., Henriksen,U., 2008. Numerical investigation of the partial oxidation in a two-stage downdraft gasifier. Fuel 87, 1383-1393.

Hawkes, A.D., Aguiar, P., Croxford, B., Leach, M.A., Adjiman, C.S., Brandon, N.P., 2007. Solid oxide fuel cell micro combined heat and power system operating strategy: Options for provision of residential space and water heating. Journal of Power Sources 164, 260–271.

http://www.ashdentrust.org.uk/PDFs/Microgen_Manifesto

http://www.energysavingtrust.org.uk/business/Global-Data/Publications/Community-heating-and-CHP

http://www.lindeengineering.com/process_plants/hydrogen_syngas_plants/gas_processing/rectisol_wash.php

http://www.opsi.gov.uk/acts/acts2004/ukpga_20040020_en_9

Janardhanan, V.M., Deutschmann, O., 2007. Numerical study of mass and heat transport in solid-oxide fuel cells running on humidified methane. Chemical Engineering Science 62, 5473-5486.

Kohl, A.L., Nielsen, R.B., 1997. Gas Purification, 5th Ed. Gulf Professional.

Koss, U., Meyer, M., 2002. Zero emission IGCC with Rectisol technology. Presentation at the GTC, San Francisco.

Kuramochi, H., Wu, W., Kawamoto, K., 2005. Prediction of the behaviours of H_2S and HCl during gasification of selected residual biomass fuels by equilibrium calculation. Fuel 84, 377–387.

Mermelstein, J., Millan, M., Brandon, N.P., 2009. The impact of carbon formation on Ni–YSZ anodes from biomass gasification model tars operating in dry conditions. Chemical Engineering Science 64, 3, 492-500.

Newby, R.A., Lippert, T.E., Slimane, R.B., Akpolat, O.M., Pandya, K., Lau, F.S., Abbasian, J., Williams, B.E., Leppin, D., 2001. Novel gas cleaning/conditioning for integrated gasification combined cycle. National Energy Technology Lab Technical Report/AC26-99FT40674-02.

Overend, R.P., Rivard, C.J., 1993. Thermal and biological gasification. First Biomass Conference of the Americas Golden Colorado, National Renewable Energy Laboratory, 47–497.

Palonen, J., Lundqvist, R.G., Stahl, K., 1995. IGCC technology and demonstration. Power Production from Biomass II VTT Symposium 164, Espoo: VTT, 41–54.

Panopoulos, K.D., Fryda, L.E., Karl, J., Poulou, S., Kakaras, E., 2006. High temperature solid oxide fuel cell integrated with novel allothermal biomass gasification Part I: Modelling and feasibility study. Journal of Power Sources 159, 570–585.

Peijun, J., Feng, W., Chen, B., 2009. Production of ultrapure hydrogen from biomass gasification with air. Chemical Engineering Science 64, 582-592.

Sadhukhan, J., Zhu, X.X., 2002. Integration Strategy of Gasification Technology: A Gateway to the Future Refining. Industrial & Engineering Chemistry Research 41(6), 1528-1544.

Shen, L., Gao, Y., Xiao, J., 2008. Simulation of hydrogen production from *biomass* gasification in interconnected fluidized beds. Biomass and Bioenergy 32, 120-127.

Smith, R. 2005. Chemical Process Design and Integration, John Wiley & Sons Ltd.

Zhao, Y. Ou, C., Chen, J., 2008. A new analytical approach to model and evaluate the performance of a class of irreversible fuel cells. International Journal of Hydrogen Energy 33, 4161 – 4170.

List of figures

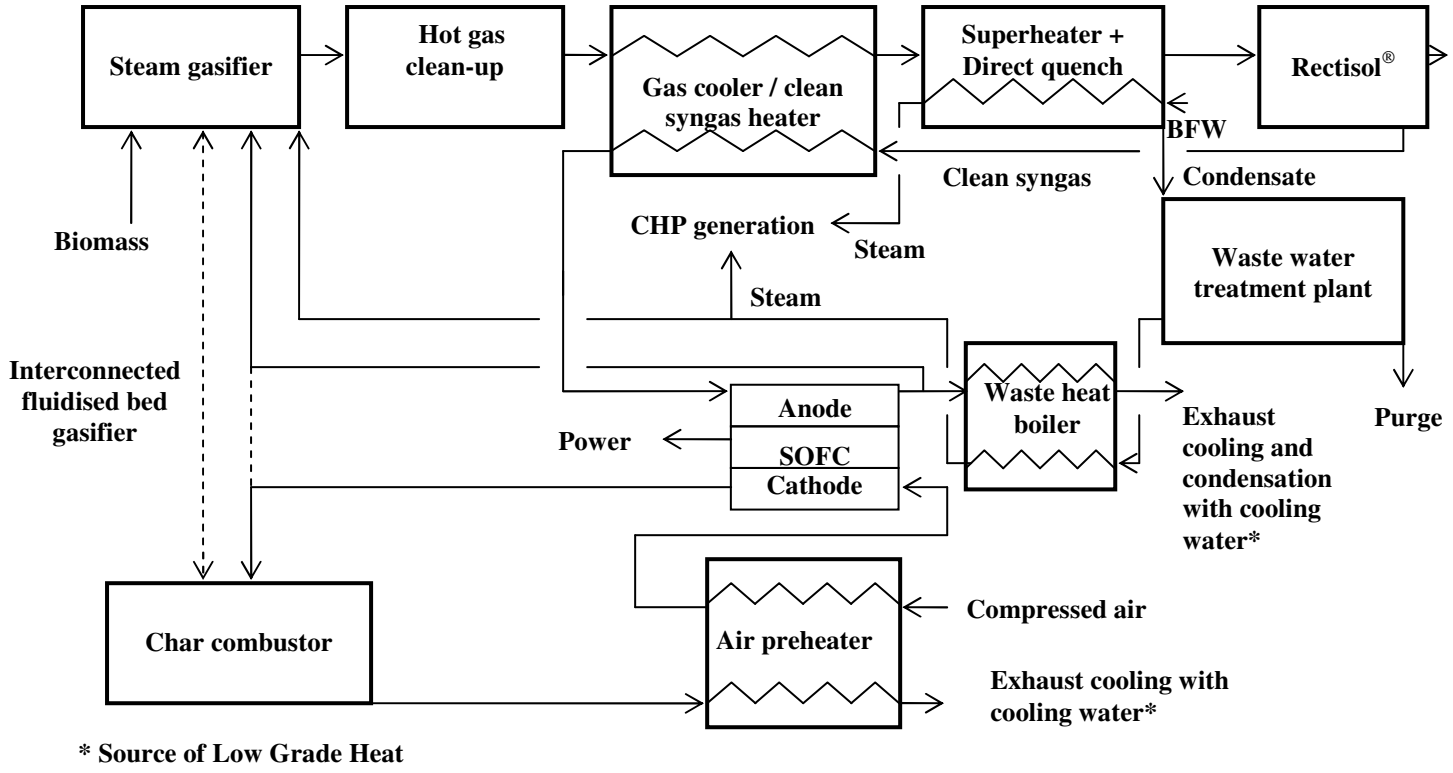

Fig. 1. Block diagram of an integrated BGFC system

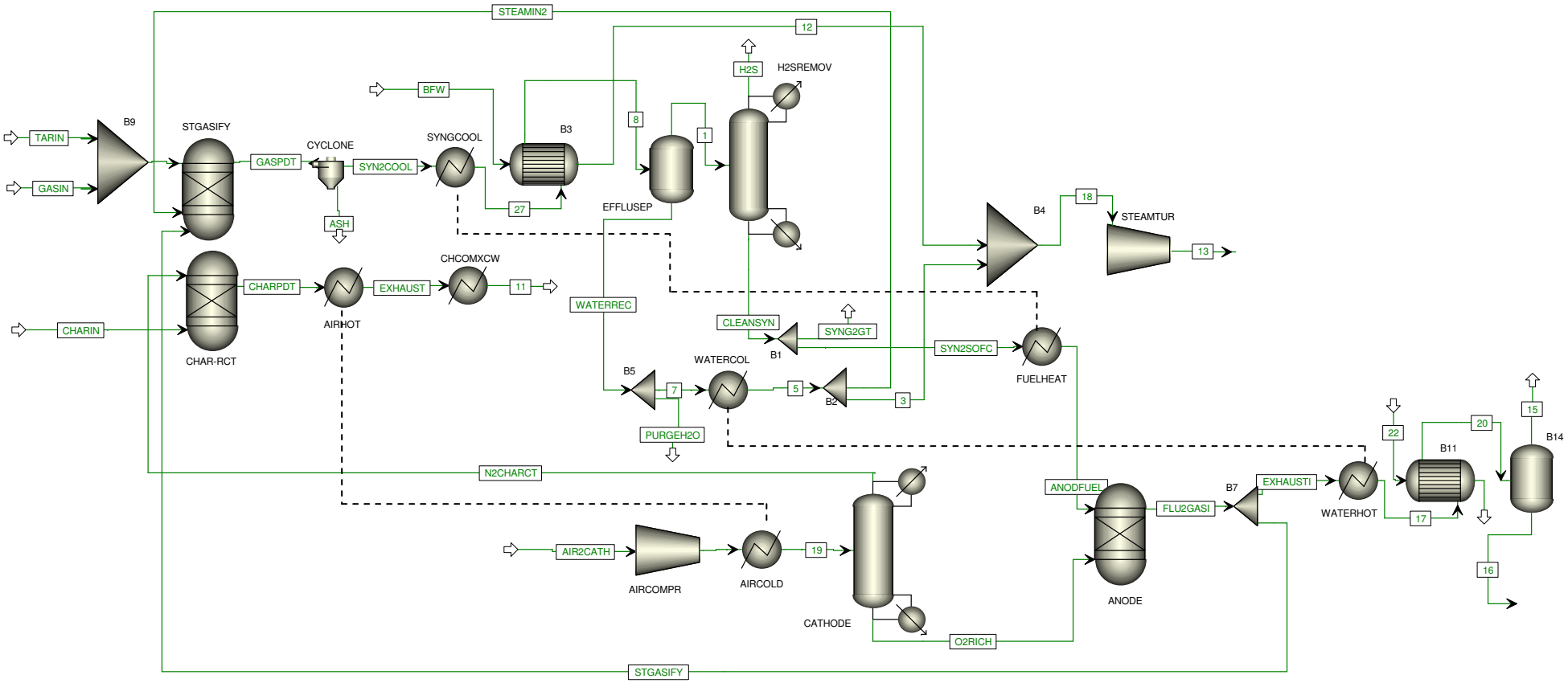

Fig. 2. Aspen simulation of material and heat integrated BGFC system

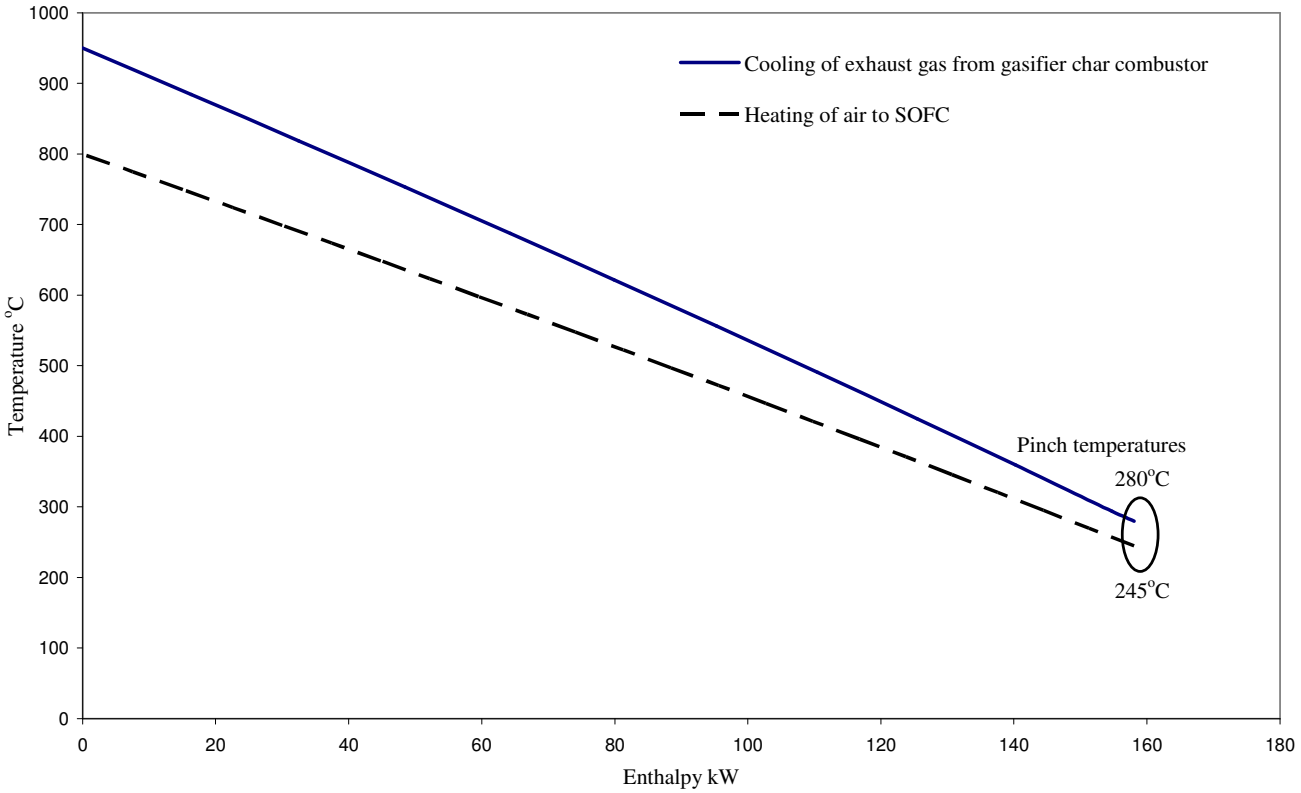

Fig. 3. Composite curves for air preheater or char combustor exhaust cooler

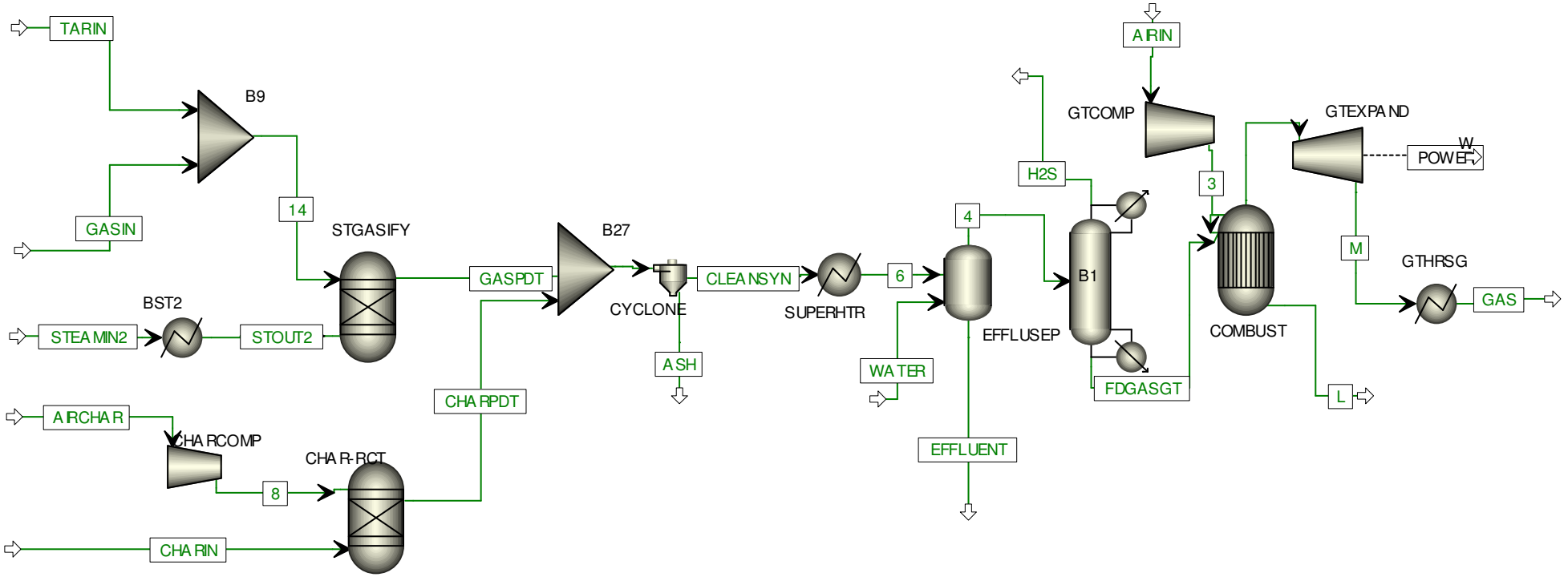

Fig. 4. Aspen simulation of material and heat integrated BGCC system

Table 1a. Ultimate analysis in wt% of straw (Shen et al., 2008)

wt%	Straw
C	36.57
H	4.91
N	0.57
O	40.70
S	0.14
Ash	8.61
Moisture	8.50
LHV MJ/kg	14.60

Table 1b. Composition of biomass (gas, tar and char) after primary pyrolysis or devolatilisation (Peijun et al., 2009)

Component	kg/kg biomass
Total devolatilization	0.9600
Total gas	0.4760
H2	0.0016
CH4	0.0241
C2	0.1227
CO	0.2164
CO2	0.0308
H2O	0.0804
Tar	Total devolatilization - total gas
Char	1-Total devolatilization

Table 2. Specifications of processes in Aspen simulation of the BGFC system (Fig. 2)

Unit names	Aspen model	Exit temperature °C	Pressure bar	Efficiency / Split fractions etc.
AIRCOLD	Heater	800	5	
AIRCOMPR	Compressor		5	75
AIRHOT	Cooler	280	1	
ANODE	RGibbs			85% fuel utilisation efficiency
B2	FSplit[1]			Flow of STEAMIN2 = 1.994 t/d
B3	HeatX[2]	Dew point of syngas		
B4	Mixer		5	
B5	FSplit[1]			PURGEH2O = 10%
B7	FSplit[1]			EXHAUSTI = 60.9%
B9	Mixer		1	
B11	HeatX[2]	Minimum approach = 20		
B14	Flash2[3]	50	1	
CATHODE	Sep2[4]			95%
CHAR-RCT	RGibbs	950	5	
CHCOMXCW	Cooler	60	1	
CYCLONE	SSplit[5]			99%
EFFLUSEP	Flash2[3]	25	1	
FUELHEAT	Heater	800	5	
H2SREMOV	Sep2[4]			99%
STEAMTUR	Turbine		1	75%
STGASIFY	RGibbs	950	5	
SYNGCOOL	Cooler	450	1	
WATERCOL	Heater	320	5	
WATERHOT	Cooler	85	1	

[1]Stream splitter based on split fraction or flows of streams etc.

[2]Heat exchanger

[3]2 component flash separator

[4]2 outlet component separator based on component purity, flow etc.

[5]Substream splitter

Table 3. Detailed Aspen simulation results of streams in the BGFC system (Fig. 2) based on straws

Stream names	GASIN	TARIN	CHARIN	ASH	GASPDT	SYN2COOL	27	8	1	CLEANSYN	SYN2SOFC	ANODFUEL	FLU2GASI	STGASIFY	EXHAUSTI	17	20	15	16
Mole Frac																			
H2O	0.228432	0.055735	0.00	0.00	0.3143806	0.3143806	0.314381	0.314381	0.031541	0.031559	0.031559	0.031559	2.92E-01	2.92E-01	2.92E-01	2.92E-01	2.92E-01	0.122607	0.992623
N2	0.011488	0	0.00	0.00	4.53E-03	4.53E-03	4.53E-03	4.53E-03	6.41E-03	6.41E-03	6.41E-03	6.41E-03	8.62E-03	8.62E-03	8.62E-03	8.62E-03	8.62E-03	0.011509	9.63E-06
O2	0	0.7629	0.00	0.00	1.48E-16	1.48E-16	1.48E-16	1.48E-16	0	0	0	0	0.0506362	0.0506362	0.0506362	0.050636	0.050636	0.067625	6.82E-05
NO2	0	0	0.00	0.00	4.25E-22	4.25E-22	4.25E-22	4.25E-22	0	0	0	0	1.35E-07	1.35E-07	1.35E-07	1.35E-07	1.35E-07	1.64E-07	4.69E-08
NO	0	0	0.00	0.00	4.93E-13	4.93E-13	4.93E-13	4.93E-13	6.97E-13	6.98E-13	6.98E-13	6.98E-13	3.79E-06	3.79E-06	3.79E-06	3.79E-06	3.79E-06	5.06E-06	1.86E-09
S	0	0.00E+00	0.00	0.00	1.57E-11	1.57E-11	1.57E-11	1.57E-11	6.93E-18	0.00E+00	0	0	1.29E-25	1.29E-25	1.29E-25	1.29E-25	1.29E-25	0	0
SO2	0	0	0.00	0.00	6.53E-09	6.53E-09	6.53E-09	6.53E-09	8.38E-09	8.38E-09	8.38E-09	8.38E-09	5.03E-05	5.03E-05	5.03E-05	5.03E-05	5.03E-05	6.47E-05	7.46E-06
SO3	0	0	0.00	0.00	3.53E-17	3.53E-17	3.53E-17	3.53E-17	0	0	0	0	2.02E-05	2.02E-05	2.02E-05	2.02E-05	2.02E-05	2.15E-05	1.64E-05
H2	0.040621	0	0.00	0.00	0.2321967	0.2321967	0.232197	0.232197	0.328699	0.328886	0.328886	0.328886	4.93E-02	4.93E-02	4.93E-02	4.93E-02	4.93E-02	6.03E-10	4.18E-14
CL2	0	0	0.00	0.00	0	0	0	0	0	0	0	0	0	0	0	0	0	0	0
HCL	0	0.00E+00	0.00	0.00	0	0	0	0	0	0	0	0	0	0	0	0	0	0	0
C	0	0.00E+00	1.00	0.00	1.30E-25	1.30E-25	1.30E-25	1.30E-25	0	0	0	0	0	0	0	0	0	0	0
CO	0.395431	0	0.00	0.00	0.2320115	0.2320115	0.232012	0.232012	0.328297	0.328484	0.328484	0.328484	4.93E-02	4.93E-02	4.93E-02	4.93E-02	4.93E-02	9.74E-10	8.69E-13
CO2	0.035822	0	0.00	0.00	0.21636	0.21636	0.21636	0.21636	0.304328	0.3045008	0.3045008	0.3045008	5.50E-01	5.50E-01	5.50E-01	5.50E-01	5.50E-01	0.798168	7.28E-03
H2S	2.46E-03	0	0.00	0.00	4.43E-04	4.43E-04	4.43E-04	4.43E-04	6.15E-04	1.00E-07	1.00E-07	1.00E-07	0	0	0	0	0	0	0
CH4	0.07689	0.00E+00	0.00	0.00	6.12E-05	6.12E-05	6.12E-05	6.12E-05	8.65E-05	8.66E-05	8.66E-05	8.66E-05	0	0	0	0	0	0	0
COS	0	0	0.00	0.00	2.02E-05	2.02E-05	2.02E-05	2.02E-05	2.76E-05	1.00E-07	1.00E-07	1.00E-07	3.68E-26	3.68E-26	3.68E-26	3.68E-26	3.68E-26	0	0
ETHAN-01	0.208854	0	0.00	0.00	1.48E-11	1.48E-11	1.48E-11	1.48E-11	2.08E-11	2.08E-11	2.08E-11	2.08E-11	0	0	0	0	0	0	0
PHENO-01	0	1.81E-01	0.00	0.00	2.08E-27	2.08E-27	2.08E-27	2.08E-27	0	0	0	0	0	0	0	0	0	0	0
Total Flow kmol/hr	4.017722	2.295644	0.68		2.27E+01	22.65893	2.27E+01	2.27E+01	16.00609	15.997	1.58E+01	15.83703	16.73088	6.541773	10.1891	10.1891	10.1891	7.626771	2.562334
Total Flow tonne/day	2.388379	2.340715	0.20	0.47	12.12515	12.12515	12.12515	12.12515	9.22849	9.221055	9.128844	9.128844	13.80937	5.399465	8.409909	8.409909	8.409909	7.290265	1.119644
Total Flow cum/hr	76.48062	42.49815			460.8679	459.7324	1362.37	646.9002	396.7779	396.5454	392.5799	282.6126	298.5633	116.7382	181.8251	303.4088	288.6615	204.9142	0.047981
Temperature °C	25	25	25.00		950	946.9866	450	70.22649	25	25	25	800	800	800	800	85	71.65806	50	50
Pressure bar	1.034214	1.034214	1.034214		5	5	1	1	1	1	1	5	5	5	5	1	1	1	1
Vapor Fraction	0.794023	0.771676			1	1	1	1	1	0.9999819	0.9999819	1	1	1	1	1	0.9882	1	0
Liquid Fraction	0.205977	0.228324			0	0	0	0	0	1.81E-05	1.81E-05	0	0	0	0	0	0.0118	0	1
Solid Fraction	0	0	1.00	1.00	0	0	0	0	0	0	0	0	0	0	0	0	0	0	0
Enthalpy kJ/mol	-145.2983	-43.76194			-152.5697	-152.565903	-172.0826	-185.3516	-163.6929	-163.775014	-163.775014	-135.86928	-284.60891	-284.60891	-284.608909	-316.2109	-317.2009	-342.8453	-284.6787
Entropy J/mol-K	-32.22472	-70.56035			56.782931	56.6599644	49.60269	23.76596	39.23541	39.1919272	39.1919272	70.90705865	34.5008104	34.50081	34.5008104	0.578345	-2.264674	5.510574	-155.7325
Density kg/cum	1.301192	2.294924	187.33	3486.88	1.096227	1.098934	0.370836	0.780979	0.96911	0.9688966	0.9688966	1.345904	1.927202	1.927202	1.927202	1.154922	1.213926	1.482385	972.2966
Average MW	24.76926	42.48481			22.29654	22.29654	22.29654	22.29654	24.02343	24.01771	24.01771	24.01771	34.39101	34.39101	34.39101	34.39101	34.39101	39.82835	18.20681
Liq Vol 60F cum/hr	0.208734	0.133462			0.9606217	0.9606217	0.960622	0.960622	0.839325	0.8388382	0.8304498	0.8304498	0.6932532	0.271062	0.4221912	0.422191	0.422191	0.37527	0.046921

Table 3 continuing

Stream names	AIR2CATH	2	19	O2RICH	N2CHARCT	CHARPDT	EXHAUST	11	WATERREC	PURGEH2O	7	5	STEAMIN2	3	BFW	12	18	13	22	25
Mole Frac																				
H2O	0	0	0	0	0	0	0	0	0.9948593	0.9948593	0.994859	0.994859	0.9948593	0.994859	1	1	0.998972	0.998972	1	1
N2	0.79	0.79	0.79	7.00E-03	0.973	0.972992	0.972992	0.972992	6.49E-06	6.49E-06	6.49E-06	6.49E-06	6.49E-06	6.49E-06	0	0	1.30E-06	1.30E-06	0	0
O2	0.21	0.21	0.21	0.993	0.027	7.52E-04	7.52E-04	7.52E-04	0	0	0	0	0	0	0	0	0	0	0	0
NO2	0	0	0	0	0	3.31E-08	3.31E-08	3.31E-08	0	0	0	0	0	0	0	0	0	0	0	0
NO	0	0	0	0	0	1.70E-05	1.70E-05	1.70E-05	3.79E-16	3.79E-16	3.79E-16	3.79E-16	3.79E-16	3.79E-16	0	0	7.59E-17	7.59E-17	0	0
S	0	0	0	0	0	0	0	0	5.34E-11	5.34E-11	5.34E-11	5.34E-11	5.34E-11	5.34E-11	0	0	1.07E-11	1.07E-11	0	0
SO2	0	0	0	0	0	0	0	0	2.09E-09	2.09E-09	2.09E-09	2.09E-09	2.09E-09	2.09E-09	0	0	4.19E-10	4.19E-10	0	0
SO3	0	0	0	0	0	0	0	0	0	0	0	0	0	0	0	0	0	0	0	0
H2	0	0	0	0	0	0	0	0	2.28E-05	2.28E-05	2.28E-05	2.28E-05	2.28E-05	2.28E-05	0	0	4.56E-06	4.56E-06	0	0
CL2	0	0	0	0	0	0	0	0	0	0	0	0	0	0	0	0	0	0	0	0
HCL	0	0	0	0	0	0	0	0	0	0	0	0	0	0	0	0	0	0	0	0
C	0	0	0	0	0	0	0	0	0	0	0	0	0	0	0	0	0	0	0	0
CO	0.00E+00	0	0	0	0	1.27E-08	1.27E-08	1.27E-08	3.59E-04	3.59E-04	3.59E-04	3.59E-04	3.59E-04	3.59E-04	0	0	7.18E-05	7.18E-05	0	0
CO2	0.00E+00	0	0	0	0	0.026239	0.026239	0.026239	4.72E-03	4.72E-03	4.72E-03	4.72E-03	4.72E-03	4.72E-03	0	0	9.44E-04	9.44E-04	0	0
H2S	0	0	0	0	0	0	0	0	3.05E-05	3.05E-05	3.05E-05	3.05E-05	3.05E-05	3.05E-05	0	0	6.10E-06	6.10E-06	0	0
CH4	0	0	0	0	0	0	0	0	2.35E-07	2.35E-07	2.35E-07	2.35E-07	2.35E-07	2.35E-07	0	0	4.71E-08	4.71E-08	0	0
COS	0	0	0	0	0	0	0	0	2.17E-06	2.17E-06	2.17E-06	2.17E-06	2.17E-06	2.17E-06	0	0	4.34E-07	4.34E-07	0	0
ETHAN-01	0	0	0	0	0	0	0	0	4.96E-13	4.96E-13	4.96E-13	4.96E-13	4.96E-13	4.96E-13	0	0	9.93E-14	9.93E-14	0	0
PHENO-01	0.00E+00	0	0	0	0	0	0	0	0	0	0	0	0	0	0	0	0	0	0	0
Total Flow kmol/hr	32.2	32.2	32.2	6.1	26.1	26.1	26.1	26.1	6.652838	0.6652838	5.987554	5.987554	4.579665	1.40789	5.63	5.63	7.03789	7.03789	3.5	3.5
Total Flow tonne/day	22.29554	22.29554	22.29554	4.68053	17.61501	17.81242	17.81242	17.81242	2.896666	0.2896666	2.607	2.607	1.994	0.613	2.434219	2.434219	3.047219	3.047219	1.51328	1.51328
Total Flow cum/hr	760.2014	277.442	574.6105	108.8548	465.7557	530.8569	1200.358	722.9489	0.121231	0.0121231	0.109108	59.05698	45.17056	13.88643	0.102088	53.67313	67.56121	257.9305	0.063465	0.066089
Temperature °C	25	245.0043	800	800	800	950	280	60	25	25	25	320	320	320	25	300.1624	304.1449	167.6413	25	65.00001
Pressure bar	1.05	5	5	5	5	5	1	1	1	1	1	5	5	5	5	5	5	1	1	1
Vapor Fraction	1	1	1	1	1	1	1	1	0	0	0	1	1	1	0	1	1	1	0	0
Liquid Fraction	0	0	0	0	0	0	0	0	1	1	1	0	0	0	1	0	0	0	1	1
Solid Fraction	0	0	0	0	0	0	0	0	0	0	0	0	0	0	0	0	0	0	0	0
Enthalpy kJ/mol	5.89E-15	6.490243	24.16061	25.24923	23.9061842	19.00973	-2.747329	-9.295856	-286.138012	-286.13801	-286.138	-232.207	-232.20705	-232.207	-285.6835	-232.2799	-232.2654	-237.0895	-285.6835	-282.8012
Entropy J/mol-K	3.976989	7.284844	30.30599	27.94918	26.6981936	31.74513	19.58232	4.507802	-161.793066	-161.79307	-161.7931	-33.24841	-33.248413	-33.24841	-162.6875	-35.05871	-34.67942	-30.82352	-162.6875	-153.6823
Density kg/cum	1.222022	3.348385	1.616717	1.791584	1.575848	1.39809	0.618304	1.026609	995.576	995.576	995.576	1.839329	1.839329	1.839329	993.5145	1.889698	1.879299	0.492256	993.5145	954.064
Average MW	28.8504	28.8504	28.8504	31.9709	28.12108	28.43624	28.43624	28.43624	18.14183	18.14183	18.14183	18.14183	18.14183	18.14183	18.01528	18.01528	18.0406	18.0406	18.01528	18.01528
Liq Vol 60F cum/hr	1.724561	1.724561	1.724561	0.326703	1.397859	1.397859	1.397859	1.397859	0.1212981	0.0121298	0.109168	0.109168	0.0834989	0.025669	0.101622	0.101622	0.127291	0.127291	0.063175	0.063175

Table 4. Comparison of CHP generations / consumptions and energy efficiency analyses between BGFC and BGCC systems

In kW	BGFC	BGCC
Power generation from SOFC based on 85% fuel efficiency	652.61	
Power generation from steam turbines	9.43	234.66
Power generation from gas turbines in BGCC system		192.00
Power consumtion by compressors	58.05	131.06
Sources of low grade heat		
WHR[1] from char combustor exhaust (CHCOMXCW in Fig. 2)	47.48	
WHR[1] from SOFC / HRSG exhaust[2]	2.8 (sensible heat) 31.18 (condensation heat)	93.57 (sensible heat)
Hot water recovered from SOFC exhaust (stream 16 in Fig. 2)[2]	1.29	
LP steam at 1 bar and 168°C (stream 13 in Table 3)	95.18	
Rectisol / Selexol process utlity consumptions		
Shaft power	0.75	
LP steam	3.33	0.75
Refrigeration duty	1.35	
Net power generation	601.89	295.60
Net heat generation	174.60	92.82
Electrical efficiency based on biomass LHV in Table 1 %	64.41	32.14
Efficiency (CHP) %	84.42	42.23
Efficiency (CHP excluding heat recovery from SOFC exhaust) %	80.65	

[1]Waste Heat Recovery

[2]Low grade heat recovery at 50°C from SOFC exhaust

Table 5. Parameters used in the SOFC electrochemical model

Parameters	Value
Operating pressure, p_0(bar)	1
Fuel composition, p_{H_2}; p_{H_2O}	0.66; 0.34*
Air composition, p_{O_2}; p_{N_2}	0.21; 0.79
Charge-transfer coefficient, β	0.5

Number of electrons, n_e	2
Pre-factor for anode exchange current density, γ_a (A/m^2)	5.5×10^8
Activation energy of anode, $E_{act,a}$ (J/mol)	1.0×10^5
Pre-factor for cathode exchange current density, γ_c (A/m^2)	7.0×10^8
Activation energy of cathode, $E_{act,c}$ (J/mol)	1.2×10^5
Electrolyte thickness, L_{el} (μ m)	20
Activation energy of O^{2-}, E_{el} (J/mol)	8.0×10^4
Pre-factor of O^{2-}, σ_0 (S/m)	3.6×10^7
Ratio of the internal resistance to the leakage resistance, k	1/100
Anode limiting current density, $i_{L,a}$ (A/m^2)	2.99×10^4
Cathode limiting current density, $i_{L,c}$ (A/m^2)	2.16×10^4
Faraday constant, F (C/mol)	96485
Universal gas constant, R (J/(mol K))	8.314
Standard molar enthalpy change at 1073K, $\Delta h°$ (J/mol)	-165204*
Standard molar entropy change at 1073K, $\Delta s°$ (J/(mol K))	-42.81*

*From Aspen simulation results in Table 3

Table 6. A comparison of stream variables and enthalpy balance between the base case in Tables 2-4 and the case with maximum recycling of steam recovered from gas cooling, to gasification

	Independent variables				Dependent variables		
	Flowrate of 3	Flowrate of STEAMIN2	Flow ratio of EXHAUSTI	WATERHOT-WATERCOL enthalpy	Temperature of 5	Concentration of ANODFUEL to SOFC	
	t/d	t/d	%	kW	^{o}C	H_2 %	CO %
Base case (Tables 2-3)		1.994	60.9	89.44	320	32.89	32.85
Maximum recycling of steam recovered from syngas, to gasification	0		74	100	500	40.88	31.85

	Energetic analysis kW						
	SOFC power	Heat of (steam) / (combustion) gasification reactions		Unutilised syngas in gasifier	Excess steam generation, 18	Low grade heat recovery from SOFC exhaust	
		Endothermic (steam)	Exothermic (combustion)	Exothermic (combustion)		From B11 and B14	Hot water 16
Base case (Table 4)	653	48.79	35.5	115.17	104.61	33.98	1.29
Maximum recycling of steam recovered from syngas, to gasification	666	57.64	35.5	118.45	79.5	50.87	1.98

Table 7. Comparison of energetic performances between straw based BGFC system for different power generations, ~ 100-1000 kW (Fig. 2)

SOFC power generation	Enthalpy	Hot side temperatures	Cold side temperatures
kW	kW	^{o}C	^{o}C
100.41	AIRHOT-AIRCOLD exchanger details		
(system operates at 2 bar)	29.5	950 (hot) and 800 (cold)	124 and 104
	WATERHOT-WATERCOL exchanger details		
	13.8	800 and 320	85 and 25
	SYNGCOOL-FUELHEAT exchanger details		
	18.95	950 and 800	450 and 25
	Waste Heat Recovery (WHR) from CHCOMXCW		
	2.097	124 and 60 (minimum)	60 and 25
	Total WHR from SOFC exhaust (B11-B14-16)		
	5.396		
	Steam at 2 bar and 246^{o}C (stream 13 in Table 3)		
	15.95		
	Power consumption by compressors and Rectisol process		
	3.22		0.32
	Electrical efficiency %		CHP efficiency %
	68.46		79.96
996.68	AIRHOT-AIRCOLD exchanger details		
(system operates at 7 bar)	218	950 (hot) and 800 (cold)	350 and 305
	WATERHOT-WATERCOL exchanger details		
	138	800 and 320	85 and 25
	SYNGCOOL-FUELHEAT exchanger details		
	189	950 and 800	450 and 25
	Waste Heat Recovery (WHR) from CHCOMXCW		
	96.5	350 and 100 (minimum)	60 and 25
	Total WHR from SOFC exhaust (B11-B14-16)		
	53.53		
	Steam at 7 bar and 320^{o}C (stream 13 in Table 3)		
	160.64		
	Power consumption by compressors and Rectisol process		
	114.27		1.38
	Electrical efficiency %		CHP efficiency %
	62.61		84.78